11-2-2005

Semiclassical Nonadiabatic Dynamics Using a Mixed Wave-Function Representation

Sophya Garashchuk
University of South Carolina--Columbia, sgarashc@chem.sc.edu

Vitaly A. Rassolov
University of South Carolina - Columbia, rassolov@chem.sc.edu

George C. Schatz
Northwestern University

Publication Info

Published in *Journal of Chemical Physics*, Volume 123, Issue 17, 2005, pages 174108-.

Semiclassical nonadiabatic dynamics using a mixed wave-function representation

Sophya Garashchuk[a)]
Department of Chemistry and Biochemistry, University of South Carolina, Columbia, South Carolina 29208 and Department of Chemistry, Northwestern University, Evanston, Illinois 60208-3113

Vitaly A. Rassolov
Department of Chemistry and Biochemistry, University of South Carolina, Columbia, South Carolina 29208

George C. Schatz
Department of Chemistry, Northwestern University, Evanston, Illinois 60208-3113

(Received 8 August 2005; accepted 7 September 2005; published online 2 November 2005)

Nonadiabatic effects in quantum dynamics are described using a mixed polar/coordinate space representation of the wave function. The polar part evolves on dynamically determined potential surfaces that have diabatic and adiabatic potentials as limiting cases of weak localized and strong extended diabatic couplings. The coordinate space part, generalized to a matrix form, describes transitions between the surfaces. Choice of the effective potentials for the polar part and partitioning of the wave function enables one to represent the total wave function in terms of smooth components that can be accurately propagated semiclassically using the approximate quantum potential and small basis sets. Examples are given for two-state one-dimensional problems that model chemical reactions that demonstrate the capabilities of the method for various regimes of nonadiabatic dynamics. © *2005 American Institute of Physics*. [DOI: 10.1063/1.2099547]

I. INTRODUCTION

Quantum effects are essential for the understanding of many chemical processes, including the behavior of large molecular systems, for which exact methods of quantum dynamics are unfeasible. In chemical reactions these effects are the most pronounced when hydrogen atoms are involved. Exact quantum-mechanical treatment, however, is often unnecessary for all degrees of freedom. A great variety of processes such as gas phase collisions, gas-surface and protein dynamics, processes in liquids, etc., are routinely studied by molecular-dynamics techniques based on classical representation of nuclei. Therefore, approximate methods incorporating quantum effects that are applicable to large molecular systems and compatible with classical molecular dynamics are highly desirable. A variety of semiclassical, quasiclassical, and other approximate methods based on classical trajectory propagation and reproducing some features of quantum-mechanical behavior have emerged over the years.

Recently, the hydrodynamic or the quantum trajectory formulation of the time-dependent Schrödinger equation[1] (SE) has received attention because of the favorable scaling with the dimensionality of a system. Following the works of Dey *et al.*[2] and Lopreore and Wyatt[3] a number of exact and approximate approaches in coordinate space[4–9] and in-phase space[10–16] have been suggested. In the quantum trajectory formulation a wave function is represented in terms of trajectories with associated phases and densities. The quantum trajectory dynamics is affected by the combined quantum and external classical potentials. This formulation gives the most compact discretized representation of wave functions, intuitive physical interpretation of quantum phenomena, and connection to classical mechanics. However, it is generally impractical for exact quantum-mechanical numerical implementation due to the possibly singular nonlocal quantum potential. Nevertheless, the quantum trajectory formulation can be viewed as a convenient starting point for approximate trajectory-based propagation methods.

In the last few years Garashchuk and Rassolov used the quantum trajectory framework to develop a well-defined, efficient, and accurate semiclassical propagation with an approximate quantum potential (AQP) determined globally from the moments of trajectory distributions.[17–20] The method scales linearly with the number of dimensions and allows for Monte Carlo sampling of the wave-function density. In its simplest form yielding a linearized quantum force, the approach is exact for Gaussian wave packets in locally quadratic potentials, which is a typical representation of moving nuclei. In more general systems it describes tunneling, zero-point energy, and isotope effects as was shown for model adiabatic chemical systems. It is desirable to advance this approach toward efficient semiclassical description of nonadiabatic
dynamics.

Nonadiabatic effects in electron-nuclear interactions play a major role in chemical reaction dynamics including reactive scattering, photochemistry, and enzymatic reactions.[21–23] Electron and proton transfers in chemical and biological systems,[24] nonradiative processes in solids and on solid surfaces such as molecular desorption and ion neutralization[25] involve several potential surfaces with transitions among them. While some nonadiabatic processes can be described

[a)]Electronic mail: sgarashc@mail.chem.sc

by the time-independent or time-dependent SE, molecular processes in laser fields with laser-induced curve crossings[26] are examples of intrinsically time-dependent nonadiabatic transition problems.

Nonadiabatic dynamics has a very long history with a great number and variety of methods based on classical treatment of nuclei combined with semiclassical or quantum treatment of electrons developed over the years. A general overview can be found in Refs. 27 and 28. Mixed quantum-classical approaches are analyzed in detail by Tully in Ref. 29. Approaches most relevant to this work are the trajectory hopping surface method and the Ehrenfest method reviewed in Ref. 29. These methods are based on an ensemble of independent classical trajectories moving on one of the potential-energy surfaces with a possibility of electronic transition in the coupling region for the former or moving on a single effective potential corresponding to the average of electronic states for the latter. In this paper we present a semiclassical description of nonadiabatic effects that is able to capture single-surface quantum effects and to generate a semiclassical nuclear wave function, as an extension of the approximate quantum potential approach. Nonadiabatic dynamics is an inherently quantum-mechanical effect that depends mostly on the separation between the electronic energy levels that are independent of nuclear masses. Therefore, we use a mixed coordinate space/polar representation of the wave function that allows us to combine elements of semiclassical and quantum-mechanical treatments.

The mixed wave-function representation was introduced to describe nodes in the density due to the initial conditions or interference within nonsingular trajectory dynamics.[30] A straightforward implementation of the quantum trajectory formulation leads to a singular quantum potential and unstable dynamics near the density nodes. Below we present equations in one dimension; multidimensional generalization in Cartesian coordinates is straightforward. The mixed representation is based on the following decomposition of the wave function

$$\psi(x,t) = \chi(x,t)\phi(x,t), \tag{1}$$

substituted into the SE. The form of Eq. (1) does not restrict the wave function and the formulation below is equivalent to the SE. The function $\phi(x,t)$ describes the overall dynamics and, once rewritten in polar form,

$$\phi(x,t) = \sqrt{\rho(x,t)}\,\exp\left(\frac{i}{\hbar}S(x,t)\right), \tag{2}$$

can be efficiently propagated in the trajectory framework. The wave-function density $\rho(x,t)$ and phase $S(x,t)$ are real functions ($\rho(x,t) \geqslant 0$). Identifying the gradient of the phase with the momentum of a trajectory, $S'(x,t)=p$, and switching to the moving frame of reference

$$\frac{d}{dt} = \frac{\partial}{\partial t} + \frac{p}{m}\frac{\partial}{\partial x}, \tag{3}$$

the trajectory position x, momentum p, and action function S evolve as in classical mechanics. This quantum trajectory is influenced by a combined potential $V+U$, where V is a classical external potential and U is the nonlocal quantum potential

$$U = -\frac{\hbar^2}{8m}(r(x,t)^2 + 2r'(x,t)), \tag{4}$$

expressed in terms of the "nonclassical" component of the momentum operator[19]

$$r(x,t) = \frac{\rho'(x,t)}{\rho(x,t)}. \tag{5}$$

Instead of the wave-function density it is convenient to use trajectory weights—the amount of density within the volume element associated with each trajectory—which is conserved for closed systems,[17]

$$w = \rho(x,t)dx_t, \quad \frac{dw}{dt} = 0. \tag{6}$$

In the semiclassical implementation the linearized nonclassical momentum $\tilde{r}(x)=r_0+r_1x$ instead of $r(x,t)$ is used. The parameters r_0, r_1 are chosen to minimize $\langle|r(x,t)-\tilde{r}(x)|^2\rangle$, which after integration by parts becomes equivalent to minimization of

$$I = \int (\tilde{r}^{\,2}x + 2\tilde{r}'\,(x))\rho(x,t)dx. \tag{7}$$

Optimized parameters define the approximate quantum potential according to Eq. (4). Evolution of $\chi(x,t)$ along a trajectory is

$$i\hbar\frac{d\chi(x,t)}{dt} = -\frac{\hbar^2}{2m}(r(x,t)\chi'(x,t) + \chi''(x,t)). \tag{8}$$

The right-hand side (rhs) of Eq. (8) is an $\hbar/m$ quantity and is small for semiclassical systems. Therefore derivatives of the initially smooth $\chi(x,t)$ can be estimated using a small real basis set $\{\eta_k(x)\}$. The approximation of $\chi'(x,t)$ as $\tilde{\chi}'(x) = \Sigma_k c_k \eta_k(x)$ conserves normalization if the coefficients $\{c_k\}$ are determined by the linear optimization of $\langle|\chi'(x,t) - \tilde{\chi}'(x)|^2\rangle$, which is equivalent to minimization of

$$I = \int (2\Re[\chi^\star(x,t)(\tilde{\chi}''(x) + r\tilde{\chi}'(x))] + |\tilde{\chi}'(x)|^2)\rho(x,t)dx, \tag{9}$$

with respect to $\{c_k\}$.

Integrals are reduced to a summation over trajectory weights once the nonclassical momentum $r(x,t)$ is replaced with its linear approximation $\tilde{r}(x)$. Alternatively, $\chi(x,t)$ itself can also be represented in terms of basis functions without approximation to the integrals since the function is known along the trajectories.

If the initial $\chi(x,0)$ is a constant, then it will remain a constant at later times and the outlined approach will be equivalent to the quantum trajectory formulation of the SE. The advantage of the mixed wave-function representation is that it can describe quantum features of the wave function, such as density nodes, while allowing for nonsingular evolution of the polar part of the wave function suitable for a semiclassical description. This concept of a mixed wave-

function representation was extended to nonadiabatic dynamics[31] with quantum trajectories on diabatic surfaces as outlined in Sec. II. Its generalization including the time evolution on dynamically determined surfaces is presented in Sec. III, followed by numerical examples and discussion in Sec. IV. Sec. V concludes.

II. TWO-COMPONENT DESCRIPTION OF NONADIABATIC EFFECTS

The simplest model of a nonadiabatic system is a wave packet evolving in the presence of two one-dimensional "electronic surfaces" V_1 and V_2 coupled by V_{12}. This system is described by a two-component wave function

$$\Psi = (\psi_1(x,t), \psi_2(x,t)), \tag{10}$$

solving the time-dependent SE for $i=1,2 (j \neq i)$

$$\left(-\frac{\hbar^2}{2m}\frac{\partial^2}{\partial x^2} + V_i - i\hbar\frac{\partial}{\partial t} \right)\psi_i(x,t) + V_{12}\psi_j(x,t) = 0. \tag{11}$$

The basic idea is to use the polar part of the wave function to represent the overall time evolution of Ψ, which can be accomplished semiclassically in an efficient manner, and to use the coordinate space part to describe the transfer of Ψ between the surfaces. In Ref. 31 this approach has been implemented by representing each component $\psi_i(x,t)$, $i=1,2$ as products of the coordinate parts and the polar parts according to Eqs. (1) and (2) with the subscript labeling surfaces. The coordinate parts $\chi_i(x,t)$ can be thought as complex "population amplitudes" that change due to the nonadiabatic coupling, though they can be also used to smooth out the polar part. The time evolution of each polar part $\phi_i(x,t)$ is equivalent to dynamics on uncoupled diabatic surfaces,

$$i\hbar\frac{\partial}{\partial t}\phi_i(x,t) = -\frac{\hbar^2}{2m}\phi_i''(x,t) + V_i\phi_i(x,t). \tag{12}$$

The time propagation is accomplished using two sets of trajectories that evolve in the presence of potentials V_1 and V_2 with the addition of the appropriate AQPs. The functions $\chi_i(x,t)$ for both surfaces are computed along the trajectories $(i=1,2, j \neq i)$

$$i\hbar\frac{d}{dt}\chi_i(x,t) = K_i\chi_i(x,t) + V_{12}\frac{\phi_j(x,t)}{\phi_i(x,t)}\chi_j(x,t). \tag{13}$$

The kinetic-energy operator K_i includes a term coupling the nonclassical momentum $r_i(x,t)=\rho_i'(x,t)/\rho_i(x,t)$ with the gradient of $\chi_i(x,t)$,

$$K_i = -\frac{\hbar^2}{2m}\left(\frac{\partial^2}{\partial x^2} + r_i(x,t)\frac{\partial}{\partial x} \right). \tag{14}$$

The rhs of Eq. (13) is evaluated by expanding $\chi_1(x,t)$ and $\chi_2(x,t)$ in a small basis set and using the linearized nonclassical momentum instead of $r_i(x,t)$ throughout. This formulation was shown to be efficient and accurate for systems with localized coupling in the diabatic representation. Nevertheless, it has a conceptual inconsistency: the coupling term in Eq. (13) is computed approximately via interpolation or expansion of $\chi_i(x,t)$, but unlike the other approximated quantities—the kinetic-energy term $K_i\chi_i(x,t)$ and the approximate quantum potential—it does not vanish in the limit of large mass. Below the mixed wave-function representation approach is generalized to avoid this approximation to the coupling terms and to choose trajectory dynamics that minimizes the effects of coupling. These features make the generalized approach efficient for any type of coupling.

III. DYNAMICALLY ADJUSTED FOUR-COMPONENT REPRESENTATION FOR NONADIABATIC SYSTEMS

Consider a system with asymptotically coupled diabatic potentials V_1 and V_2, such as often occurs in collisions of an open shell atom such as $O(^3P)$ with a close shell molecule. The standard approach in this case is to use the adiabatic representation which results in asymptotically uncoupled dynamics. The wave function Ψ solving Eq. (11) and the adiabatic function Ψ^a are related by the transformation

$$\Psi = M^{-1}\Psi^a. \tag{15}$$

The transformation matrix M is a coordinate-dependent function,

$$M = \begin{pmatrix} \cos\theta(x) & \sin\theta(x) \\ -\sin\theta(x) & \cos\theta(x) \end{pmatrix}, \tag{16}$$

where the angle $\theta(x)$,

$$\theta(x) = \frac{1}{2}\arctan\frac{2V_{12}}{V_1 - V_2}, \tag{17}$$

diagonalizes the potential matrix V,

$$V = \begin{pmatrix} V_1 & V_{12} \\ V_{12} & V_2 \end{pmatrix}. \tag{18}$$

The dynamics of Ψ^a is governed by the adiabatic potentials,

$$V_i^a = \tfrac{1}{2}(V_1 + V_2 + (-1)^i\sqrt{(V_2 - V_1)^2 + 4V_{12}^2}). \tag{19}$$

Transitions between two adiabatic surfaces occur due to localized derivative coupling.

We propose a four-component representation of Ψ in terms of the coordinate and polar parts which has the structure of Eq. (15) but which allows us to *find* a convenient, dynamically adjusted form of Ψ,

$$\Psi = \begin{pmatrix} \chi_{11}(x,t) & \chi_{12}(x,t) \\ \chi_{21}(x,t) & \chi_{22}(x,t) \end{pmatrix}\begin{pmatrix} \phi_1(x,t) \\ \phi_2(x,t) \end{pmatrix}. \tag{20}$$

Setting $\hbar=1$ below, the time evolution of $\phi_1(x,t)$ and $\phi_2(x,t)$ is governed by so far unspecified potentials $\tilde{V}_1$ and $\tilde{V}_2$,

$$i\hbar\frac{\partial}{\partial t}\phi_j(x,t) = -\frac{1}{2m}\phi_j''(x,t) + \tilde{V}_j\phi_j(x,t). \tag{21}$$

Substitution of Eq. (20) into Eq. (11) gives the following expressions for $\chi_{ij}(x,t)$, $j=1,2$:

$$\sum_{i=1,2}\left(i\frac{d}{dt}\chi_{ij}(x,t) - u_{ij} \right)\phi_j(x,t) = 0, \tag{22}$$

where, with the definitions (14) and (18),

$$u_{ij} = K_j\chi_{ij}(x,t) + \sum_{k=1,2} V_{ik}\chi_{kj}(x,t) - \tilde{V}_j\chi_{ij}(x,t). \tag{23}$$

The functions $\chi_{11}(x,t)$ and $\chi_{21}(x,t)$ are defined along trajectories evolving under the influence of $\tilde{V}_1$ (trajectory set I); the full time derivative for the quantities associated with set I is given by Eq. (3) with $p=p_1$. Similarly, the functions $\chi_{12}(x,t)$ and $\chi_{22}(x,t)$ are defined along trajectories evolving in the presence of $\tilde{V}_2$ (trajectory set II); the full time derivative for the quantities of set II is given by Eq. (3) with $p=p_2$.

Without loss of generality Eq. (22) can be rewritten in an *uncoupled* form by subtracting and adding an arbitrary function $F_i(x,t)$,

$$i\frac{d}{dt}\chi_{ij}(x,t) = u_{ij} + (-1)^j\frac{F_i(x,t)}{\phi_j(x,t)}. \tag{24}$$

The function $F_i(x,t)$ determines the contributions to $\psi_i(x,t)$ from the two sets of trajectories as elaborated below. This is a crucial step that allows computation of $\chi_{ij}(x,t)$ to be performed locally, i.e., along each trajectory.

Equations (20), (21), and (24) are equivalent to the original SE (11) provided $\phi_i(x,t)\neq 0$. This formulation offers a lot of flexibility—the functions $F_i(x,t)$, propagation potentials $\tilde{V}_i$, and the initial conditions of $\chi_{ij}(x,t)$ and $\phi_j(x,t)$ are not unique. These functions are chosen to yield the limit of smooth $\chi_{ij}(x,t)$ and Gaussian $\phi_j(x,t)$, where this formulation becomes exact. However, it is also possible to choose the unspecified functions to recover two-component dynamics on diabatic and adiabatic surfaces. We examine the limiting cases of coupled dynamics for typical initial wave function—at time $t=0$ the wave packet is located on the first surface, $\Psi(x,0)=(\psi_1(x,0),0)$.

A. Dynamics on diabatic surfaces

Assume that the dynamics of $\phi_j(x,t)$ proceeds on the diabatic surfaces, $\tilde{V}_j=V_j$. Then, the initial conditions consistent with single surface dynamics in the absence of coupling is

$$\begin{pmatrix}\chi_{11}(x,0) & \chi_{12}(x,0)\\ \chi_{21}(x,0) & \chi_{22}(x,0)\end{pmatrix} = \begin{pmatrix}1 & 0\\ 0 & 0\end{pmatrix}, \tag{25}$$

and $\phi_1(x,0)=\psi_1(x,0)$. The choice of $F_1(x,t)=-V_{12}\chi_{22}(x,t)\phi_2(x,t)$ and $F_2(x,t)=V_{12}\chi_{11}(x,t)\phi_1(x,t)$ ensures that $\chi_{12}(x,t)$ and $\chi_{21}(x,t)$ remain zero in the course of the dynamics. Therefore, the four-component formulation reduces to the earlier two-component form of Eqs. (12) and (13) with $\chi_1(x,t)=\chi_{11}(x,t)$ and $\chi_2(x,t)=\chi_{22}(x,t)$.

For the chosen initial condition, $\psi_2(x,0)=0$ and $\chi_{22}(x,0)=0$, the initial $\phi_2(x,0)$ is, formally, arbitrary. In practice, one needs $\phi_1(x,t)$ and $\phi_2(x,t)$ to have significant overlap in the coupling region in order to ensure smooth $\chi_{ij}(x,t)$ and $F_i(x,t)$. The simplest choice for the initial $\phi_2(x,0)$ is to take it identical to $\phi_1(x,0)$. This is the condition used in the examples below. In general, the initial condition can be adjusted to maximize overlap in the coupling region: the initial $\phi_2(x,0)$ can be taken as the result of a single surface propagation of $\phi_1(x,0)$ using V_1 into the coupling region followed by propagation back in time up to $t=0$ under the influence of V_2.

B. Dynamics on adiabatic surfaces

Suppose that a given system is described in the adiabatic representation: the functions $\phi_j(x,t)$ evolve according to adiabatic potentials given by Eq. (18) and components of Ψ^a are equivalent to $\phi_j(x,t)$. Then, the functions $\chi_{ij}(x,t)$ should be equivalent to the respective components of the inverse transformation matrix, $\chi_{ij}(x,t)=M^{-1}_{ij}$. Using these $\chi_{ij}(x,t)$, $\tilde{V}_j$, and the identity $\tan\theta=\sin 2\theta/(1+\cos 2\theta)$ the potential terms in Eq. (24) simplify to give zero. Since the chosen $\chi_{ij}(x,t)$ are time independent, Eq. (24) does not have a solution for a general V_{12}. Therefore, the kinetic-energy terms from Eq. (24), $K_j\chi_{ij}(x,t)$, should be included into Eq. (21). This rearrangement recovers the SE (11) rewritten in terms of the adiabatic wave function $\Psi^a=(\phi_1(x,t),\phi_2(x,t))$.

If the diabatic surfaces are degenerate, then there should be a four-component formulation without transfer of the wave-function density between the components associated with $\phi_1(x,t)$ and $\phi_2(x,t)$, i.e., $F_i(x,t)=0$. Formally, in this case the M^{-1} transformation does not give derivative coupling terms since $\theta'(x)=0$. The functions $\chi_{ij}(x,t)$ remain constant throughout the propagation if the dynamics proceeds on the adiabatic surfaces for unique initial conditions

$$\begin{pmatrix}\chi_{11}(x,0) & \chi_{12}(x,0)\\ \chi_{21}(x,0) & \chi_{22}(x,0)\end{pmatrix} = \frac{1}{2}\begin{pmatrix}1 & 1\\ -1 & 1\end{pmatrix}. \tag{26}$$

C. Dynamically defined four-component formulation

1. Potentials $\tilde{V}_1, \tilde{V}_2$

For general nonadiabatic problems we would like to have some intermediate diabatic/adiabatic propagation where the effect of the coupling is the smallest. At the level of an approximate implementation, we specify the arbitrary functions, $\tilde{V}_1,\tilde{V}_2,F_1(x,t),F_2(x,t)$ in such a way that $\chi_{ij}(x,t)$ remains smooth throughout the propagation. This is consistent with the semiclassical regime where $K_j\chi_{ij}(x,t)$ is small and $\chi_{ij}(x,t)$ is well represented using a small number of trajectories. Spatial oscillations in $\chi_{ij}(x,t)$ arise mostly due to the potential terms in Eq. (24). Therefore, the propagation potentials $\tilde{V}_j$ are defined to minimize these terms. Taking $\tilde{V}_j$ as a linear combination of potential surfaces,

$$\tilde{V}_j = c_{1j}V_1 + c_{2j}V_2 + c_{3j}V_{12}, \tag{27}$$

gives the simplest form of the potential which reproduces purely diabatic and adiabatic dynamics. The coefficients which cancel the individual contributions of V_1,V_2,V_{12} in Eq. (24) on average are

$$c_{kj} = \langle |\chi_{kj}(x,t)|^2 \rangle / N_j, \; k = 1,2,$$
$$c_{3j} = 2\Re \langle \chi_{1j}^*(x,t) \chi_{2j}(x,t) \rangle / N_j. \tag{28}$$

N_j is the average density associated with the jth set of trajectories

$$N_j = \sum_i \langle |\chi_{ij}(x,t)|^2 \rangle. \tag{29}$$

Average values involving $\chi_{ij}(x,t)$ are computed using the density $\rho_j(x,t)$. V_1, V_2, V_{12}, playing role of weighting functions were omitted in the integrals for c_{1j}, c_{2j}, c_{3j}, respectively. Other more rigorous but more expensive minimization procedures of the rhs of Eq. (24) can also be defined. The potentials $\tilde{V}_j$ somewhat resemble the effective potential of the Ehrenfest method. However, the mixed representation approach is quite different from the mean-field type methods in that: (i) trajectories representing the wave function are coupled and the single-surface quantum-mechanical effects can be reproduced; (ii) there are as many effective potentials $\tilde{V}_j$ as there are electronic states; (iii) the wave-function density is defined by population amplitudes $\chi_{ij}(x,t)$ along with the trajectory weights, so that unphysical outcomes are, in principle, precluded. Moreover, it is possible to define $\tilde{V}_{ij}$ by averaging on subspaces,[20] within specific reaction channels, rather than on entire space. This will eliminate the unphysical influence of the spatially separated wave-function components.

2. Reexpansion and initial conditions

Formally, the contributions to the components of Ψ from different sets of trajectories in Eq. (24) are coupled by unspecified functions $F_i(x,t)$. If these are set to zero, then one effectively arrives at the two-component formulation of Eqs. (12) and (13) with identical polar parts, $\phi_2(x,t) = \phi_1(x,t)$. Implementation of this procedure is very cheap since all quantities are known along the same trajectory unlike the formulation with two sets of trajectories. This framework is well suited for dynamics during which $\psi_1(x,t)$ and $\psi_2(x,t)$ have significant overlap in the interaction region. Otherwise, it will be inefficient, since $|\chi_{ij}(x,t)|$ can be large in regions of small density $\rho_j(x,t)$.

Ideally, we would like $F_i(x,t)$ to give the optimal, in a sense of smoothness of $\chi_{ij}(x,t)$, partitioning of $\psi_j(x,t)$ between $\phi_1(x,t)$ and $\phi_2(x,t)$. In order to achieve this there should be an "exchange" of the transferred parts between $\chi_{21}(x,t)$ and $\chi_{22}(x,t)$ and between $\chi_{11}(x,t)$ and $\chi_{12}(x,t)$. Instead of defining such a mechanism as part of the dynamics, $F_i(x,t)$ in Eq. (24) is eliminated and a reexpansion procedure for $\chi_{11}(x,t)$ and $\chi_{12}(x,t)$ is introduced,

$$\psi_1(x,t) = \tilde{\chi}_{11}(x,t)\phi_1(x,t) + \tilde{\chi}_{12}(x,t)\phi_2(x,t),$$
$$\tilde{\chi}_{1j}(x,t) = \chi_{1j}(x,t) + (-1)^j F \phi_j^{-1}(x,t). \tag{30}$$

The functional form of F is independent of which component of $\Psi(x,t)$ is reexpanded. Reexpansion of $\psi_2(x,t)$ is completely analogous to that for $\psi_1(x,t)$. Analyzing the solution for $\chi_{1j}(x,t)$ with $1/m$ terms neglected, and assuming that exchange occurs if $\phi_1(x,t)$ and $\phi_2(x,t)$ have significant overlap and that all the terms have the same dimensionality, we arrive at the following form for F:

$$F = (\rho_1(x,t)\rho_2(x,t))^{1/4}(\alpha e^{iS_2(x,t)} - \beta e^{iS_1(x,t)}). \tag{31}$$

A form of the new functions that is convenient for trajectory implementation is

$$\tilde{\chi}_{11}(x) = \chi_{11}(x) + r_{21}(x)(\beta - \alpha\sigma(x)),$$
$$\tilde{\chi}_{12}(x) = \chi_{12}(x) + r_{12}(x)(\alpha - \beta\sigma^*(x)), \tag{32}$$

where $\sigma(x) = \exp(iS_2(x,t) - iS_1(x,t))$ and $r_{ij}(x) = (\rho_i(x,t)/\rho_j(x,t))^{1/4}$. The parameters α and β are chosen so that the new functions are close to being constants γ_{1j}, i.e., that $\{\alpha, \beta, \gamma_{11}, \gamma_{12}\}$ minimize

$$I = \langle |\tilde{\chi}_{11}(x) - \gamma_{11}|^2 \rangle + \langle |\tilde{\chi}_{12}(x) - \gamma_{12}|^2 \rangle. \tag{33}$$

The quantities $r_{ij}(x)$ and $\sigma(x)$ involve an amplitude and phase of $\phi_1(x,t)$ and $\phi_2(x,t)$ at the same point, which can be approximated using linearized nonclassical momenta to estimate $\rho_j(x,t)$ and linearized classical momenta to obtain a quadratic fit to $S_j(x,t)$. The minimization is linear and requires computation of just the first and second moments of x and p from the trajectory distribution.

The reexpansion also deals with the ambiguity of the initial conditions for $\chi_{ij}(x,t)$. This procedure converts physically reasonable initial values of $\chi_{ij}(x,t)$ into the matrices (25) or (26) for systems with small diabatic and adiabatic couplings, respectively. In the intermediate regime reexpansion makes the final result independent of the initial choice of $\chi_{ij}(x,t)$, as demonstrated in the next section.

IV. NUMERICAL EXAMPLES

We apply the generalized mixed representation strategy to problems modeling different regimes of nonadiabatic dynamics studied in Ref. 32, which has become the standard test for approximate and semiclassical propagation methods[33] and to the intersystem crossing model of Ref. 34.

A. Simple avoided crossing

The first system examined is a simple avoided crossing (model A) (Ref. 32) with localized coupling. Previously this system was treated using the two-component formulation given by Eqs. (12) and (13) with two sets of diabatic trajectories.[31] The energy-resolved transmission probabilities were obtained using the wave-packet correlation formulation for the scattering matrix:[35] this approach allows one to obtain probabilities for a range of energies from a single propagation, but it is quite sensitive to errors in the correlation function. The setup and potential are shown in Fig. 1(a). The initial wave packet is localized on the lower surface V_1 in the asymptotic region of the reactant channel. It is propagated toward the coupling region. Its reactive part reaches the asymptotic product region, where the two surfaces separate. The diabatic threshold for the reaction is at 52.5 kJ/mol. Results for high energies, $E > 100$ kJ/mol, were in very good

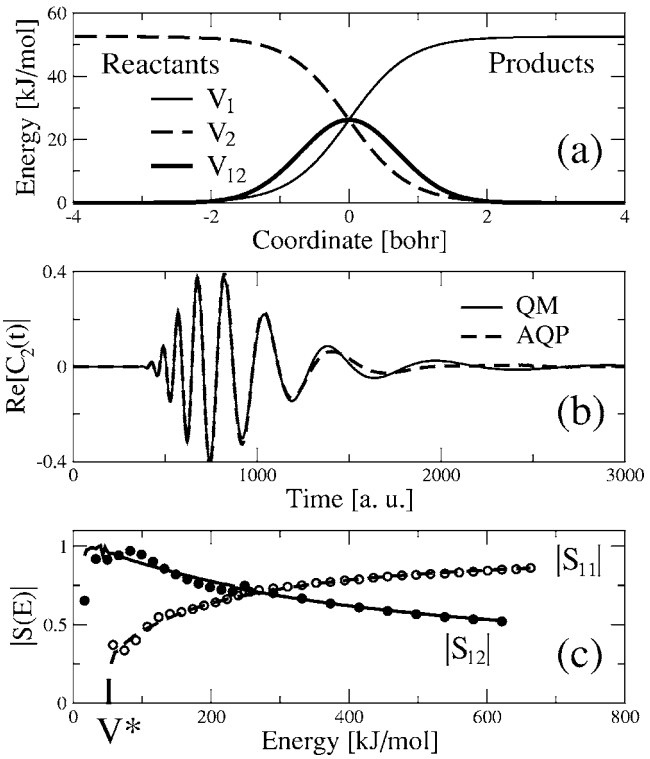

FIG. 1. Dynamics and reaction probabilities. (a) Diabatic potentials and coupling. (b) The real parts of the quantum (solid line) and AQP (dashed line) correlation functions, $C_2(t)$, for the reaction with electronic transition. (c) The energy-resolved scattering matrix amplitudes for the reaction on V_1, $|S_{11}|$, and for the reaction with transition to V_2, $|S_{12}|$: quantum result is shown with the dashed and solid line for the two processes, respectively; the corresponding AQP results are shown with open and filled circles, respectively; $V^\star$ marks the threshold of the reaction on the diabatic surface V_1.

agreement with quantum results. The low-energy probabilities, influenced by the resonances, were underestimated in the semiclassical calculation.

While the trajectory calculation was performed very efficiently with just a few hundred trajectories per wave packet, it required estimation of the functions $\chi_1(x,t)$, $\phi_1(x,t)$ associated with the trajectories on surface V_1 at the positions of trajectories on the surface V_2 and vice versa. This evaluation step is entirely avoided in the formulation involving a single set of trajectories moving on the effective potential given by Eq. (27). Though the concept of the effective potential has mean-field flavor, the current approach is formally equivalent to the time-dependent SE for the exact $\chi_{1j}(x,t)$ and $\phi_j(x,t)$.

The mixed representation without reexpansion is computationally efficient, since the $\chi_{1j}(x,t)$ are known along the same set of trajectories. The only quantities that have to be estimated is the kinetic energy from Eq. (14) $K_1\chi_{i1}(x,t)$ for $i=1,2$. We repeat the transmission probability calculation of Ref. 31 using Gaussian initial wave packets

$$\psi_1(x,0)=\left(\frac{2a_0}{\pi}\right)^{1/4}\exp(-a_0(x-x_0)+ip_0(x-x_0)). \quad (34)$$

The parameter values in a.u. are $a_0=12$, $x_0=-2.35$, and $p_0=25$ for the high-energy wave packet and $p_0=13$ for the low-energy wave packet. Initial conditions for the mixed formulation are $\phi_1(x,0)=\psi_1(x,0)$, $\chi_{11}(x,0)=1$, and $\chi_{21}(x,0)=0$. Functions associated with the second set of trajectories, $\chi_{12}(x,t)$ and $\chi_{22}(x,t)$, remain zero for all time. The high-energy wave packet was propagated up to $t=800$ a.u. using 399 trajectories and the low-energy wave packet was propagated up to $t=3000$ a.u. using 799 trajectories. Correlation functions $C_i(t)$ of $\psi_i(t)$ overlapping a symmetrically placed stationary wave packet (34) with $x_0=2.35$ bohr and the same a_0,p_0 as in $\psi_1(x,0)$ are computed by finding $\psi_j(x,t)$ at 31 points as a convolution with a narrow Gaussian function. Kinetic-energy terms are estimated from the linear approximation to $\chi_i'(x,t)$. The real part of the correlation function $C_2(t)$ for the low-energy wave packet is shown in Fig. 1(b). It agrees quite well with the quantum result at intermediate times, but falls off faster than the quantum result at long times, which is also the case for $C_1(t)$. Correlation functions for the high-energy wave packet are in good agreement with the quantum result and are not shown. Figure 1(c) shows the scattering matrix elements, $|S_{11}(E)|$ and $|S_{12}(E)|$ for scattering from V_1 to V_1 and to V_2, respectively. The agreement in the high-energy regime is quantitative; the low-energy regime has some discrepancy but is still in good overall agreement with the quantum result.

We also tested the four-component formulation with reexpansion and found no improvement compared to the single set of trajectories, probably because asymptotically all potentials are constants and dynamics on surfaces $\tilde{V}_1$ and $\tilde{V}_2$ is essentially the same. Therefore, we conclude that the formulation with one set of trajectories is suitable for systems with large overlaps $\langle\psi_1(x,t)|\psi_2(x,t)\rangle$ in the coupling region. The approach is numerically efficient and sufficiently accurate in the semiclassical regime.

B. Weak asymptotic coupling

Next we consider a system with asymptotically degenerate surfaces that remain weakly coupled in the product region in the diabatic representation. The model was designed by Hoffmann and Schatz[34] as part of studies of the spin-orbit induced intersystem crossing in SH_2. The diabatic potentials and coupling shown on Fig. 2(a) are given by

$$V_1=\frac{A}{1+\exp(-ax)}+\frac{B}{4\cosh^2(ax/2)},$$

$$V_2=\Delta+\frac{C}{1+\exp(-ax)}+\frac{D}{4\cosh^2(ax/2)}, \quad (35)$$

$$V_{12}=sA(1+\tanh(x+h)).$$

Parameter values and mass of the particle m are given in Table I.

Since V_1 and V_2 are asymptotically degenerate, nonadiabatic dynamics can be efficiently described with the single set of trajectories. Apart from cheap propagation this has the advantage that expectation values in both diabatic and adiabatic representations can be computed directly. The wave-packet reaction probabilities P_{11} and P_{12} from the reactant region of surface V_1 to the product region of the adiabatic surfaces V_1^a and V_2^a, are found by summing over the reactive trajectories at some large value of time t,

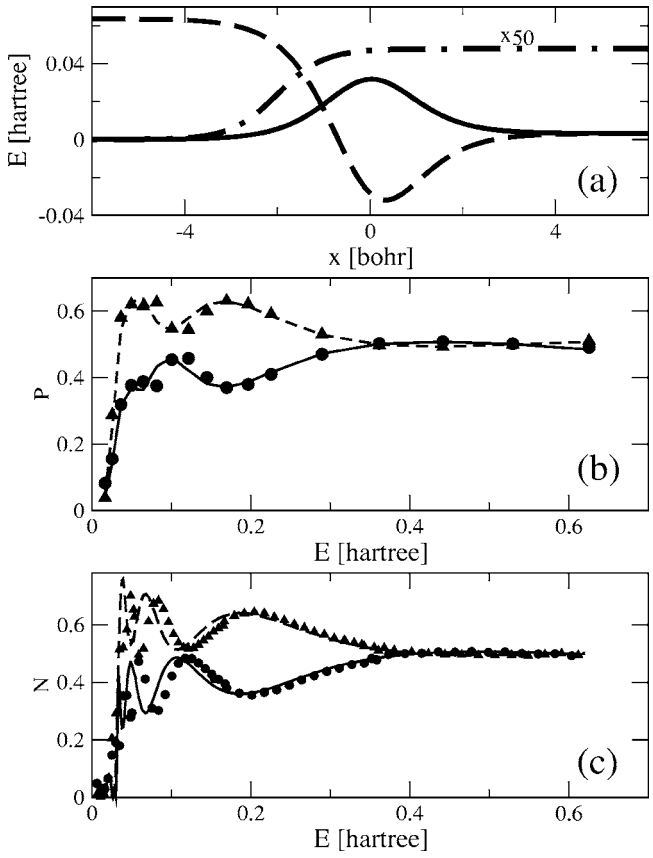

FIG. 2. Weak extended coupling. (a) Potential surfaces, V_1 (solid line), V_2 (dashed), and coupling V_{12} (dot-dashed). (b) The wave-packet probabilities as a function of the initial energy of the wave packet: quantum mechanical P_{11} and P_{12} are shown with solid line and dashed, respectively; semiclassical P_{11} and P_{12} are shown with circles and triangles, respectively. (c) The energy-resolved probabilities. Legend is the same as in (b).

$$P_{1j} = \lim_{t\to\infty} \langle \Psi_j^a(x,t) | h(x-q) | \Psi_j^a(x,t) \rangle = \sum_{x_l > q} |\Psi_j^a(x_l,t)|^2 w_l. \tag{36}$$

The index l labels trajectories. The adiabatic functions $\Psi_j^a, j=1,2$ are defined by Eq. (15). The function $h(x-q)$ is the Heaviside function. Reaction probabilities for the initial Gaussian wave packet (34) with parameters $a_0=2$, $x_0=5$, and $p_0=[8,50]$ in a.u. are shown on Fig. 2(b). Trajectories were considered reactive if $x_l(t)$ exceeded $q=4$ bohrs. Wave packets were propagated using 199 trajectories until P_{1j} reached a constant value. The agreement with the quantum result is quite good especially at high energies, $E>0.15$ hartree.

We also computed a phase sensitive quantity—the energy-resolved reaction probabilities from the wave-packet correlation functions, $C_j(t)=\langle \Psi_j(x,t) | \Psi_0(x,0) \rangle$, computed for four reactant wave packets, $\Psi_1(x,0)$, with initial parameters $a_0=12$, $x_0=-7$. Initial momenta and propagation times are listed in Table I. The stationary product wave packets $\Psi_0(x,0)$ had the same width and momenta as $\Psi_1(x,0)$ and centered at $x_0=7$ bohrs. The energy-resolved reaction probabilities were obtained from the Fourier transform of $C_j(t)$ normalized with respect to energy as was done in Ref. 31. Note that because of the asymptotic coupling, the scattering matrix is defined in terms of adiabatic energy eigenstates. Therefore, the energy normalization of the product wave packet is shifted by the asymptotic values of adiabatic potentials V_j^a, Eq. (18). Semiclassical calculation of the correlation function required from 400 trajectories for the high-energy wave packets to 1600 trajectories for the low-energy wave packets. The number of trajectories can be reduced by improved sampling of initial conditions as was done in Ref. 17. The reaction probabilities $N(E)$ for the adiabatic and nonadiabatic processes are shown on Fig. 2(c). The Stueckelberg oscillations due to interference of multiple pathways to the same final state,[36] are well described by the semiclassical approach. The agreement for the high-energy regime is quantitative. In the low-energy regime semiclassical probabilities exhibit a nonuniform shift in energy compared to the quantum result, while capturing the overall behavior of $N(E)$. The reason for this discrepancy is that at low energies the system is not semiclassical: the effect of the kinetic energy of the χ components becomes large and the approximate quantum potential is less accurate. This was verified by linearizing $\chi'_{ij}(x,t)$ and the nonclassical momentum on subspaces rather than on the entire space.[20] With this modification that will be detailed elsewhere, the trajectory approach gave accurate probabilities.

C. Extended coupling with reflection

While the first two model problems are well described within the two-component formulation, we take full advantage of the four-component representation to treat the system with extended coupling, model C in Ref. 32. This regime dominated by the coupling is considered to be more difficult for semiclassical methods. The diabatic potentials are constants with the splitting $V_2-V_1=1.2\times10^{-3}$ hartree, which is small compared to the asymptotic value of 0.2 hartree for the coupling V_{12}. The system is usually treated in the adiabatic representation. The setup is sketched on Fig. 3. Both of our two-component approaches are inefficient for this model.

TABLE I. Parameters for the weak extended coupling model in a.u.

Model parameters							
A	B	C	D	Δ	a	s	m
0.003 187	0.121 022	−0.060 553	−0.246 584	0.063 74	1.5	0.15	1732
Initial momentum, p_0				Propagation time			
I	II	III	IV	I	II	III	IV
12	20	30	40	5000	3000	1500	1500

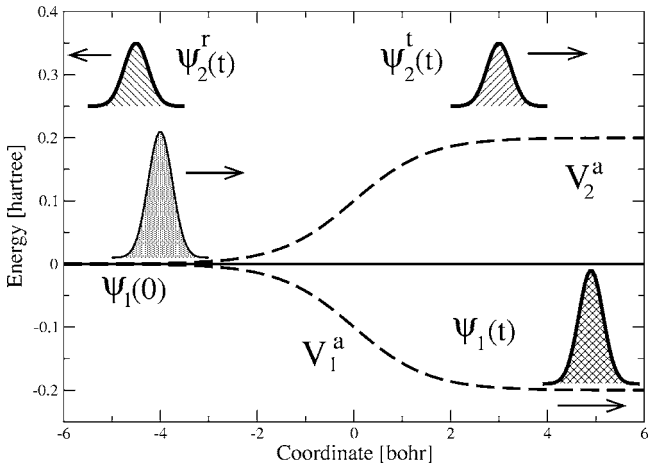

FIG. 3. Extended coupling with reflection. Adiabatic potential surfaces V_1^a and V_2^a are shown with dashed lines; diabatic potential surfaces shown with a single solid line have a small splitting of 1.2×10^{-3} hartree.

The earlier formulation based on diabatic surface dynamics are expensive (i) because of the transitions in the coupled asymptotic region and (ii) because χ components are large due to the mismatch of coupled and uncoupled dynamics on diabatic surfaces. The formulation with the single set of trajectories in the averaged potential is cheap but χ components are still expected to be large since the lower and upper adiabatic surfaces have large splitting and the dynamics on these two surfaces can be qualitatively different. The reexpansion procedure becomes essential for representing Ψ in terms of smooth functions $\chi_{ij}(x,t)$ and $\phi_j(x,t)$.

We start with the wave packet on the lower surface given by Eq. (34) with the parameter values $a_0=8$, $x_0=-4$, and $p_0=20$ in a.u. Initial conditions for the polar parts of the wave functions are $\phi_1(x,0)=\phi_2(x,0)=\psi_1(x,0)$. We find that regardless of the choice of initial $\chi_{ij}(x,t)$ the four components become close to the adiabatic condition (26) after several time steps with reexpansion. One of the components, $\chi_{11}(x,t)$, for three sets of initial conditions is shown in Fig. 4. The starting values of $\chi_{11}(x,0)$ were chosen 0.999, 0.75, and 0.5. The other components were taken as $\chi_{12}(x,0)=1-\chi_{11}(x,0)$, $\chi_{22}(x,0)=\chi_{12}(x,0)$, and $\chi_{21}(x,0)=-\chi_{22}(x,0)$. The

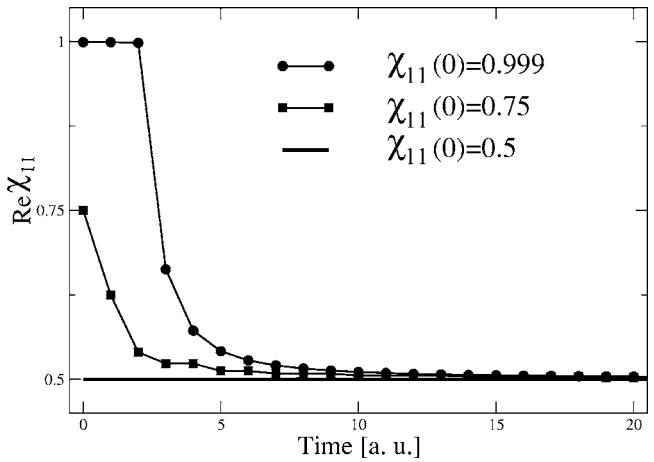

FIG. 4. Real part of χ_{11} as a function of time for three values of initial conditions for the extended coupling model.

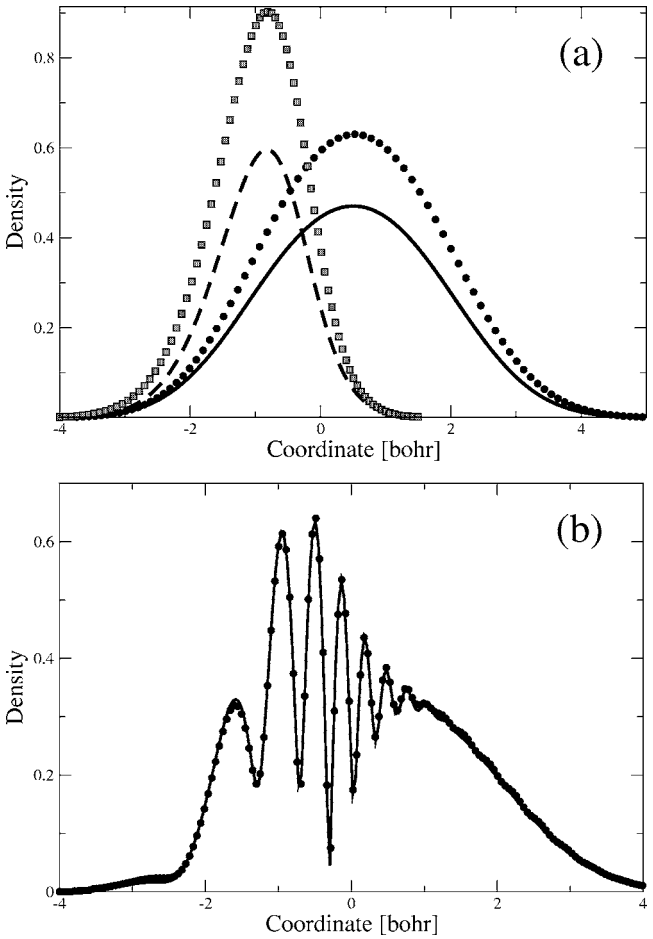

FIG. 5. Wave-function density for $t=500$ a.u. (a) Quantum-mechanical wave-function density in adiabatic representation for ψ_1^a (solid line) and ψ_2^a (dashed), and the semiclassical polar density for ϕ_1 (circle) and ϕ_2 (square) at $t=500$ a.u. (b) Quantum-mechanical (line) and semiclassical (circles) wave-function densities in the diabatic representation.

reexpansion procedure generates adiabatic conditions for $\chi_{ij}(x,t)$ for $t>10$ for all three choices of the initial conditions. The propagation potentials $\tilde{V}_j$ given by Eq. (27) are very close to adiabatic potentials $\tilde{V}_j\approx(-1)^jV_{12}$.

Let us examine the wave function at time $t=500$ a.u., which corresponds to the middle of the reaction. Figure 5(a) shows quantum-mechanical wave-function amplitudes in the adiabatic representation compared to the amplitudes of semiclassical $\phi_j(x,t)$. The dynamics of $\phi_j(x,t)$, which is normalized to one, is very similar to the dynamics of the exact Ψ in the adiabatic representation, therefore $\chi_{ij}(x,t)$ remains smooth during the propagation. The full wave function in the diabatic representation is shown on Fig. 5(b). The amplitude exhibits a strong oscillatory pattern due to the interference of $\psi_1(x,t)$ and $\psi_2(x,t)$ caused by coupling. This effect will not be reproduced using approximate quantum trajectories on diabatic potentials.

V. CONCLUSIONS

We have generalized the mixed wave-function representation approach in conjunction with a quantum trajectory propagation method to describe nonadiabatic dynamics, with emphasis on applications modeling chemical reactions. The

wave function in the diabatic representation is treated as a sum of contributions from wave packets moving on the dynamically adjusted potential surfaces. These wave packets when rewritten in polar form in terms of amplitude and phase, are described semiclassically using trajectory-based methods that have favorable scaling with system size. This is essential for a broad goal of studying quantum-mechanical effects on the dynamics of nuclei in large molecular systems. The inherently quantum effect of electronic transitions is described in coordinate space in terms of a matrix of complex "population amplitudes." The number of the polar components and the size of the matrix are equal to the number of electronic states. The quantum trajectory formulation gives the most local formulation (at the expense of losing linear properties) of the SE. All quantities defining the wave function can be computed along the trajectories except for the nonclassical momentum, $r(x,t)=\rho'(x,t)/\rho(x,t)$. This nonlocal quantity defines the quantum potential which vanishes in the semiclassical limit of large m. The mixed representation is designed to achieve the same goal—to have a description of nonadiabatic wave functions that becomes local in the semiclassical limit. The effective potentials for the trajectories and partitioning of the total wave function between different polar components are chosen to minimize nonlocality, or the spatial derivatives, of the coordinate part. The kinetic-energy terms associated with the coordinate part of the wave function vanish in the limit of large mass as is the case for the quantum potential. The potentials governing the trajectories are defined as a linear combination of diabatic interactions weighted by the average population amplitudes associated with the corresponding polar part. This particular form is the simplest one consistent with the limit of vanishing coupling in the diabatic and adiabatic representations. The reexpansion is designed to minimize the deviation from the average of the population amplitudes and to eliminate the effect of their initial choice when propagating the wave function approximately. Overall, the method is set up in such a way that all nonlocal information is obtained from the first and second moments of the trajectory distribution that leads to favorable scaling properties with the system size.

This approach was applied to three two-state models testing different regimes of nonadiabatic dynamics. We find that for systems with localized coupling or weak asymptotic coupling the formulation without reexpansion is adequate in the semiclassical regime. Being based on propagation of a single set of trajectories, it is the cheapest implementation of the mixed representation approach. We obtained the energy-resolved probabilities using the wave-packet correlation function formulation of the scattering matrix. The high-energy reaction probabilities agree with the quantum results quite well as expected from the semiclassical regime. In the quantum low-energy regime probabilities are less accurate due to approximation to the kinetic energy of χ_{ij} and to the quantum potential. Both of these approximations can be improved upon by using subspaces for approximation of the nonlocal quantities.[20] In principle, the approach with subspaces can be taken to the limit of full quantum mechanics. In the third model of strong extended coupling with reflection the reexpansion procedure is crucial for the semiclassical description. It leads to a decomposition of the diabatic wave function in terms of smooth wave packets moving on adiabatic surfaces. The interference pattern of the diabatic wave functions is accurately reproduced which was impossible with the straightforward implementation of the quantum trajectory formalism or with just two population amplitudes.

We have demonstrated that the generalized mixed representation approach is well suited for description of nonadiabatic dynamics for typical test problems. The approach was implemented with the quantum trajectories, but other semiclassical trajectory propagation methods can be used as well. More rigorous procedures for defining potentials and reexpansion can also be introduced. Further studies and applications are needed for a more complete evaluation of the approach, including coupling induced by the ultrashort laser pulses[37] and multidimensional and multistate systems. This approach shows a promise for including nonadiabatic and single-surface quantum effects into large scale molecular-dynamics simulations.

ACKNOWLEDGMENTS

Acknowledgment is made to the Donors of the American Chemical Society Petroleum Research Fund and to the Chemistry Division of NSF for support of this research.

[1] D. Bohm, Phys. Rev. **85**, 166 (1952).
[2] B. K. Dey, A. Askar, and H. Rabitz, J. Chem. Phys. **109**, 8770 (1998).
[3] C. L. Lopreore and R. E. Wyatt, Phys. Rev. Lett. **82**, 5190 (1999).
[4] E. R. Bittner, J. Chem. Phys. **112**, 9703 (2000).
[5] R. E. Wyatt and E. R. Bittner, J. Chem. Phys. **113**, 8898 (2000).
[6] B. K. Kendrick, J. Chem. Phys. **119**, 5805 (2003).
[7] D. Babyuk and R. E. Wyatt, J. Chem. Phys. (in press).
[8] B. Poirier, J. Chem. Phys. **121**, 4501 (2004).
[9] J. Liu and N. Makri, J. Phys. Chem. A **108**, 5408 (2004).
[10] I. Burghardt and L. S. Cederbaum, J. Chem. Phys. **115**, 10303 (2001).
[11] I. Burghardt and L. S. Cederbaum, J. Chem. Phys. **115**, 10312 (2001).
[12] I. Burghardt and K. B. Moller, J. Chem. Phys. **117**, 7409 (2002).
[13] J. B. Maddox and E. R. Bittner, J. Phys. Chem. B **106**, 7981 (2002).
[14] E. R. Bittner, J. B. Maddox, and I. Burghardt, Int. J. Quantum Chem. **89**, 313 (2002).
[15] A. Donoso and C. C. Martens, Phys. Rev. Lett. **87**, 223202 (2001).
[16] C. J. Trahan and R. E. Wyatt, J. Chem. Phys. **119**, 7017 (2003).
[17] S. Garashchuk and V. A. Rassolov, J. Chem. Phys. **118**, 2482 (2003).
[18] S. Garashchuk and V. A. Rassolov, Chem. Phys. Lett. **376**, 358 (2003).
[19] S. Garashchuk and V. A. Rassolov, J. Chem. Phys. **120**, 1181 (2004).
[20] V. A. Rassolov and S. Garashchuk, J. Chem. Phys. **120**, 6815 (2004).
[21] L. J. Butler, Annu. Rev. Phys. Chem. **49**, 125 (1998).
[22] L. Sun, K. Song, and W. L. Hase, Science **296**, 875 (2002).
[23] S. C. Ammal, H. Yamataka, M. Aida, and M. Dupuis, Science **299**, 1555 (2003).
[24] *Electron Transfer in Inorganic, Organic and Biological Systems*, edited by J. R. Bolton, N. Mataga, and G. McLendon (American Chemical Society, Washington, DC, 1991).
[25] R. Engleman, *Non-radiative Decay of Ions and Molecules in Solids* (North-Holland, Amsterdam, 1979).
[26] R. J. Gordon and S. A. Rice, Annu. Rev. Phys. Chem. **48**, 601 (1997).
[27] A. Donoso, D. Kohen, and C. C. Martens, J. Chem. Phys. **112**, 7345 (2000).
[28] C. L. Lopreore and R. E. Wyatt, J. Chem. Phys. **116**, 1228 (2002).
[29] J. C. Tully, in *Modern Methods for Multidimensional Dynamics Computations in Chemistry*, edited by D. Thompson (World Scientific, Singapore, 1998), pp. 34–72.
[30] S. Garashchuk and V. A. Rassolov, J. Chem. Phys. **121**, 8711 (2004).
[31] V. A. Rassolov and S. Garashchuk, Phys. Rev. A **71**, 032511 (2005).
[32] J. C. Tully, J. Chem. Phys. **93**, 1061 (1990).

[33] X. Sun and W. H. Miller, J. Chem. Phys. **106**, 6346 (1997).
[34] M. R. Hoffmann and G. C. Schatz, in *Low-lying Potential Energy Surfaces*, ACS Symposium Series, Vol. 828 (American Chemical Society, 2002), pp. 329–345.
[35] D. J. Tannor and D. E. Weeks, J. Chem. Phys. **98**, 3884 (1993).
[36] E. E. Nikitin, *Theory of Elementary Atomic and Molecular Processes in Gases* (Clarendon, Oxford, 1974).
[37] F. Grossmann, Phys. Rev. A **60**, 1791 (1999).